ACCELERATION OF AN ITERATIVE METHOD FOR THE EVALUATION OF HIGH-FREQUENCY MULTIPLE SCATTERING EFFECTS*

YASSINE BOUBENDIR[†], FATIH ECEVIT[‡], AND FERNANDO REITICH[§]

Abstract. High frequency integral equation methodologies display the capability of reproducing single-scattering returns in frequency-independent computational times and employ a Neumann series formulation to handle multiple scattering effects. This requires the solution of an enormously large number of single-scattering problems to attain a reasonable numerical accuracy in geometrically challenging configurations. Here we propose a novel and effective Krylov subspace method suitable for the use of high frequency integral equation techniques that significantly accelerates the convergence of Neumann series. We additionally complement this strategy utilizing a preconditioner based upon Kirchhoff approximations that provides a further reduction in the overall computational cost.

Key words. Helmholtz equation, high frequency, multiple scattering, integral equations, Krylov subspace, Kirchhoff approximations

AMS subject classifications. 45A05, 65N38, 78M35

DOI. 10.1137/16M1080501

1. Introduction. In the last two decades significant advances have taken place in the realm of computational scattering with notable theoretical as well as practical contributions in the domains of finite elements [29, 17, 9] and integral equations [12, 4, 8, 36, 11]. However, simulation strategies based upon the former are usually restricted to low and mid frequency applications. Indeed, use of finite element methods in exterior scattering simulations requires not only utilization of an artificial interface to truncate the infinite computational domain but also introduction of appropriate absorbing boundary conditions on this interface to effectively replicate the behavior of solution at infinity [6, 21, 26, 27, 28]. Recently some new methodologies have been proposed in [22, 35, 37] to effectively solve the issues related to large frequencies. However, these difficulties are further amplified on models involving multiple scatterers, such as the one treated in the present paper, because the distance that separates the obstacles naturally increases the size of the truncated domain. Integral equation methods, in contrast, are more adequate for these situations since, on the one hand, they explicitly enforce the radiation condition by simply choosing an appropriate outgoing fundamental solution and, on the other hand, they are solely based on the knowledge of solution confined only to the scatterers. This, in return, provides a dimensional reduction in the computational domain for surface scattering applications [16]. Nevertheless, they deliver dense linear systems whose sizes increase in proportion to k^p with increasing wavenumber k, where p is the dimension of the computational manifold.

^{*}Submitted to the journal's Computational Methods in Science and Engineering section June 20, 2016; accepted for publication (in revised form) September 5, 2017; published electronically December 6, 2017.

http://www.siam.org/journals/sisc/39-6/M108050.html

Funding: The first author's work was supported by the NSF through grants DMS-1319720 and DMS-1720014.

[†]Department of Mathematical Sciences, New Jersey Institute of Technology, University Heights, Newark, NJ 07102 (boubendi@njit.edu).

[‡]Department of Mathematics, Boğaziçi University, Bebek TR 34342, Istanbul, Turkey (fatih. ecevit@boun.edu.tr).

[§]CAP S.A., Gertrudis Echeñique 220, Santiago, Chile (fernando.reitich@cap.cl).

Broadly speaking, the success of integral equation approaches in high-frequency simulations is directly linked with the incorporation of asymptotic characteristics of the unknown into the solution strategy. This is essentially the path we follow in this manuscript, since it transforms the problem into the determination of a new unknown whose oscillations are virtually independent of frequency. The pioneering work in this direction is due to Nedéléc and co-authors [1, 2] who, in two-dimensional simulations, have provided a reduction from $\mathcal{O}(k)$ to $\mathcal{O}(k^{1/3})$ in the number of degrees of freedom needed to obtain a prescribed accuracy. What has had a significant impact is the single-scattering algorithm of Bruno et al. [13] (based on a combination of Nyström method, extensions of the method of stationary phase, and a change of variables around the shadow boundaries—the points where the rays are tangential to the boundary) as it has demonstrated the possibility of $\mathcal{O}(1)$ solution of surface scattering problems. (See [10] for a three-dimensional variant.) Alternative implementations of this approach built on collocation and geometrical theory of diffraction [24], collocation, and steepest descent [32] and a p-version Galerkin interpretation [18] have later appeared. In this latter setting, Ecevit and Ozen [19] have recently developed a rigorous method which demands, for any smooth convex scatterer, an increase of $\mathcal{O}(k^{\epsilon})$ (for any $\epsilon > 0$) in the number of degrees of freedom to maintain a prescribed accuracy independent of frequency.

The single-scattering algorithm [13] has been successfully extended by Bruno, Geuzaine, and Reitich [14] to encompass the high-frequency multiple scattering problems considered in this paper, relating precisely to a finite collection of smooth, strictly convex obstacles. Roughly speaking, the approach in [14] was based on the following: (1) representation of the overall solution η (namely, the normal derivative of the total field in acoustics and the surface current in electromagnetics) as an infinite superposition of single scattering effects through use of a Neumann series that takes on the form $\eta = \sum_{m=0}^{\infty} \eta^m$, where η^m corresponds exactly to the waves that have undergone precisely m geometrical reflections; (2) determination of the phase associated with each one of these effects using a spectral geometrical optics solver wherein the assumption that the obstacles are smooth and strictly convex ensures that the phase functions are single valued; and (3) utilization of the high-frequency single scattering algorithm [13] for the frequency independent evaluation of these effects. While every numerical implementation in [14] has displayed the spectral convergence of Neumann series for two smooth strictly convex obstacles, unfortunately, a rigorous proof of this fact was not available. Indeed, we have later shown for several smooth convex obstacles in both two- [20] and three-dimensional [5] settings that the Neumann series can be rearranged into contributions associated with primitive periodic orbits and an explicit rate of convergence formula can be rigorously derived on each periodic orbit in the high-frequency regime. While, on the one hand, these analyses depict the convergence of Neumann series for all sufficiently large wavenumbers k, on the other hand, the rate of convergence formulas display that convergence can be rather slow particularly when (at least) one pair of nearby obstacles exists. This analysis of the rate convergence [20, 5] was performed by using double layer potentials. In this work, we show that use of combined field integral equations lead to the same rate of convergence. Accordingly, novel mechanisms are much needed for the accelerated solution of multiple scattering problems that retain the frequency independent operation count underlying the algorithm in [14]. However, this is a rather challenging task since the algorithm in [14] undeviatingly rests on reducing the problem, at each iteration, to the computation of an unknown with a single-valued phase, and thus any strategy aimed at accelerating the convergence of Neumann series must also preserve the phase information related with the iterates.

In this paper, we develop a Krylov subspace method that significantly accelerates the convergence of Neumann series, in particular in the case where the distance between obstacles decreases, hence deteriorating the rate of convergence. For instance, in [25] the authors design an efficient multiple scattering algorithm for Maxwell's equations but also discuss the difficulties arising when the distance between the obstacles is small. The method we propose herein is well adapted to the high frequency aspect of the present problem as it retains the phase information associated with the iterates and delivers highly accurate solutions in a small number of iterations. Note specifically that a direct implementation of Krylov subspace methods inhibits the use of the algorithm in [14] as this makes it impossible to track the phase information of the corresponding iterates. As we shall see, a natural attempt to overcome this issue would be to simply use the binomial formula; however, this disrupts the convergence of the method as displayed in the numerical results. We defeat this additional difficulty by introducing an alternative numerically stable decomposition of the iterates. In summary, our approach is based on three main elements: (1) utilization of an appropriate formulation of the multiple scattering problem in the form of an operator equation of the second kind, (2) alternative representation of the associated Krylov subspaces so as to guarantee that basis elements are single-phased and thus retain the frequency independent operation count underlying the algorithm in [14], and (3) a novel decomposition of the iterates entering in a (standard) Krylov recursion to prevent instabilities that would otherwise arise in a typical implementation based on binomial identity. Indeed, as depicted in our numerical implementations, the resulting methodology is immune to numerical instabilities as it removes the additive cancellations arising from a direct use of binomial theorem. Moreover, it provides additional savings in the number of needed iterations when compared with the classical Padé approximants used in [14].

We additionally complement our Krylov subspace approach utilizing a preconditioner based upon Kirchhoff approximations to further reduce the number of iterations needed to obtain a given accuracy. Indeed, since knowledge of the illuminated regions—where the inner product of the incidence direction and the exterior surface normal is negative—at each iteration is readily available through the geometrical optics solver we have used to precompute the phase of multiple scattering iterations, essentially the only additional computation needed for the application of this preconditioner is the use of stationary phase method to deal with nonsingular integrals wherein the only stationary points are the target ones. This kind of dynamical preconditioning is unusual and its originality resides in the fact that the location of illuminated regions varies at each reflection. This clearly distinguishes our preconditioning strategy from classical approaches where the preconditioners are usually steady by design.

While the success of this Kirchhoff preconditioner is clearly displayed in our numerical tests, the utilization of Kirchhoff approximations for the multiple scattering iterations naturally raises the question of convergence of the associated Neumann series. We address this problem by showing that this series converges for each member of a general general class of functions, and explain the exact sense in which the spectral radius of the Kirchhoff operator is strictly less than 1. The importance of this result is twofold. First, it verifies that the multiple scattering problem can be solved by using solely the Kirchhoff technique, and further it rigorously answers the validity of our preconditioning strategy.

The rest of the paper is organized as follows. In section 2, we introduce the scattering problem and provide a comparison of the equivalent differential and integral equation formulations of multiple scattering problems. Section 3 is reserved for a comparison of convergence characteristics of these approaches. In section 4, we provide a short review of the algorithm in [14] as the ideas therein lie at the core of frequency independent evaluation of multiple scattering iterations as well as the iterates associated with our newly proposed Krylov subspace method detailed in section 5. In section 6, we explain how this Krylov subspace approach can be preconditioned while utilizing Kirchhoff approximations. Finally, in section 7, we present numerical implementations validating our newly proposed methodologies.

2. Scattering problem and multiple scattering formulations. Given an incident field u^{inc} satisfying the Helmholtz equation in \mathbb{R}^n (n=2,3), we consider the solution of sound-soft scattering problem

(1)
$$\begin{cases} \left(\Delta + k^2\right) u = 0 & \text{in } \mathbb{R}^n \backslash \Omega, \\ u = -u^{\text{inc}} & \text{on } \partial \Omega, \\ \lim_{|x| \to \infty} |x|^{(n-1)/2} \left(\partial_{|x|} - ik\right) u(x) = 0 \end{cases}$$

in the exterior of a smooth compact obstacle $\Omega \subset \mathbb{R}^n$. Potential theoretical considerations entail that [16] the *scattered field u* satisfying (1) admits the single-layer representation

$$u(x) = -\int_{\partial K} \Phi(x, y) \, \eta(y) \, ds(y),$$

where

$$\eta = \partial_{\nu} \left(u + u^{\rm inc} \right) \quad \text{on } \partial\Omega$$

is the unknown normal derivative of the total field (called the surface current in electromagnetics), ν is the exterior unit normal to $\partial\Omega$,

$$\Phi(x,y) = \begin{cases} \frac{i}{4} H_0^{(1)}(k|x-y|), & n=2, \\ \frac{1}{4\pi} \frac{e^{ik|x-y|}}{|x-y|}, & n=3, \end{cases}$$

is the fundamental solution of the Helmholtz equation, and $H_0^{(1)}$ is the Hankel function of the first kind and order zero. Although η can be recovered through a variety of integral equations [16], we use the uniquely solvable *combined field integral equation* (CFIE)

(2)
$$\eta(x) - \int_{\partial\Omega} (\partial_{\nu(x)} + ik) G(x, y) \eta(y) ds(y) = f(x), \quad x \in \partial\Omega,$$

where $G = -2\Phi$ and $f(x) = 2(\partial_{\nu(x)} + ik) u^{\text{inc}}(x)$.

In case the obstacle Ω consists of finitely many disjoint subscatterers $\Omega_1, \ldots, \Omega_J$, denoting the restrictions of η and f to $\partial \Omega_j$ by η_j and f_j so that

(3)
$$\eta = (\eta_1, \dots, \eta_J)^t \quad \text{and} \quad f = (f_1, \dots, f_J)^t,$$

(2) gives rise to the coupled system of integral equations

$$(4) (\mathcal{I} - \mathcal{S}) \eta = f,$$

where

$$\left(\mathcal{S}_{jj'}\eta_{j'}\right)(x) = \int_{\partial\Omega_{j'}} \left(\partial_{\nu(x)} + ik\right) G(x,y) \,\eta_{j'}(y) \, ds(y), \qquad x \in \partial\Omega_{j}.$$

In connection with the operator $\mathcal{I} - \mathcal{S}$, the following result will be useful in extending our two-dimensional results in [20] concerning the convergence of multiple scattering iterations to the case of CFIE.

THEOREM 1. For each k > 0, the diagonal operator $\mathcal{D} = \operatorname{diag}(\mathcal{I} - \mathcal{S}) : L^2(\partial\Omega) \to L^2(\partial\Omega)$ defined by

 $\mathcal{D}_{jj'} = \left\{ \begin{array}{cc} \mathcal{I}_j - \mathcal{S}_{jj} & \textit{if } j = j', \\ 0 & \textit{otherwise} \end{array} \right.$

is continuous with a continuous inverse. Moreover, if each Ω_j is star-like with respect to a point in its interior, then given $k_0 > 0$ there exists a constant $C_{k_0} > 0$ such that

(5)
$$\|\mathcal{D}^{-1}\|_2 \le C_{k_0}$$

for all $k \geq k_0$.

Proof. This is immediate since \mathcal{D} is a diagonal operator and, as shown in [15, Theorem 4.3], each operator $\mathcal{I} - \mathcal{S}_{jj}$ (j = 1, ..., J) on its diagonal satisfies inequality (5).

Multiplying (4) with the inverse of \mathcal{D} yields the equivalent operator equation of the second kind

(6)
$$(\mathcal{I} - \mathcal{T}) \eta = g,$$

where

(7)
$$\mathcal{T}_{jj'} = \begin{cases} 0, & j = j', \\ (\mathcal{I} - \mathcal{S}_{jj})^{-1} \mathcal{S}_{jj'}, & j \neq j', \end{cases}$$

and

$$g = (g_1, \dots, g_J)^t$$

with $g_j = (\mathcal{I} - \mathcal{S}_{jj})^{-1} f_j$. Under suitable restrictions on the geometry of scatterers, the solution of the operator equation (6) is given by the Neumann series [20, 5]

(8)
$$\eta = \sum_{m=0}^{\infty} \eta^m,$$

where the multiple scattering iterations

(9)
$$\eta^m = (\eta_1^m, \dots, \eta_I^m)^t$$

are defined by

(10)
$$\eta^m = \begin{cases} g, & m = 0, \\ \mathcal{T}\eta^{m-1}, & m \ge 1. \end{cases}$$

As was presented in [7], the multiple scattering problem described above possesses an equivalent differential equation formulation. Naturally, the convergence analysis carried out in [7] is directly linked with that of the Neumann series (8) and here we present the exact connection. Indeed, the fields u_j given by the single-layer potentials

$$u_j(x) = -\int_{\partial\Omega_j} \Phi(x, y) \, \eta_j(y) \, ds(y)$$

in connection with the components of η in (3) correspond precisely to the unique solutions of the exterior sound-soft scattering problems

$$\begin{cases} \left(\Delta + k^2\right) u_j = 0 & \text{in } \mathbb{R}^n \backslash \Omega_j, \\ u_j = -u^{\text{inc}} - \sum_{j' \neq j} u_{j'} & \text{on } \partial \Omega_j, \\ \lim_{|x| \to \infty} |x|^{(n-1)/2} \left(\partial_{|x|} - ik\right) u_j(x) = 0, \end{cases}$$

and they provide the decomposition of the scattered field u as

$$(11) u = \sum_{j=1}^{J} u_j.$$

On the other hand, the iterated fields u_i^m given by the single-layer potentials

(12)
$$u_j^m(x) = -\int_{\partial\Omega_j} \Phi(x, y) \, \eta_j^m(y) \, ds(y)$$

in relation with the components of η^m in (9) are precisely the unique solutions of the exterior sound-soft scattering problems

$$\begin{cases} \left(\Delta + k^2\right) u_j^m = 0 & \text{in } \mathbb{R}^n \backslash \Omega_j, \\ u_j^m = -h_j^m & \text{on } \partial \Omega_j, \\ \lim_{|x| \to \infty} |x|^{(n-1)/2} \left(\partial_{|x|} - ik\right) u_j^m(x) = 0 \end{cases}$$

with

$$h_j^m = \begin{cases} u^{\text{inc}}, & m = 0, \\ \sum_{j' \neq j} u_{j'}^{m-1}, & m \geq 1, \end{cases}$$

and thus, in case the Neumann series (8) converges, each solution u_j can be expressed as the superposition

$$(13) u_j = \sum_{m=0}^{\infty} u_j^m.$$

3. Convergence of multiple scattering iterations. Preliminary work on the justification of identity (13) in a three-dimensional setting has appeared in [7]. Indeed, while [7, Theorem 1] establishes uniqueness of decomposition (11), [7, Theorem 3] justifies the convergence of the series in (13) under suitable restrictions on the geometry of the obstacles Ω_i as stated in the next theorem.

THEOREM 2 (cf. [7]). Assume that $u^{\text{inc}} \in H^1(\partial\Omega)$ and, for $j = 1, \ldots, J$, the obstacle Ω_j is nontrapping in the sense that

$$\beta_j = \frac{1}{\operatorname{diam}(\Omega_j)} \sup_{y \in \Omega_j} \inf_{x \in \partial \Omega_j} \nu(x) \cdot (x - y) > 0.$$

Let

$$\delta = \max_{1 \le j \le J} \operatorname{diam}(\Omega_j), \quad d = \min_{1 \le j, j' \le J} \operatorname{dist}(\Omega_j, \Omega_{j'}), \quad |\partial \Omega| = surface \ area \ of \ \partial \Omega.$$

Then there exists a constant $\beta > 0$ that depends on β_1, \ldots, β_J such that if

$$\frac{\delta d^2}{|\partial \Omega|} \beta > k^3 \left(1 + (\delta k)^2 \right) \sqrt{1 + 2 (\delta k)^2},$$

then, for j = 1, ..., J, identity (13) holds in the sense of convergence in $H^1_{loc}(\mathbb{R}^n \backslash \Omega_j)$.

As is clear, Theorem 2 establishes convergence of the series (13) for nontrapping obstacles only if the wavenumber k is sufficiently small. Work on rigorous justification of the convergence of Neumann series (8) (and thus of identity (13)) in high-frequency applications, on the other hand, reduces to our work [20] and [5] that relates to a finite collection of smooth strictly convex (and thus nontrapping in the sense of Theorem 2) obstacles in two and three dimensions, respectively. Indeed, as we have shown in [20, 5], the Neumann series (8) can be rearranged into a sum over primitive periodic orbits and a precise (asymptotically geometric) rate of convergence \mathcal{R}_p (where p is the period of the orbit), which depends only on the relative geometry of the obstacles Ω_i , can be derived on each periodic orbit in the asymptotic limit as $k \to \infty$.

To review these results, for the sake of simplicity of exposition, we assume that the scatterer Ω consists only of two smooth strictly convex obstacles Ω_1 and Ω_2 in which case there are only two (primitive) periodic orbits (initiating from each Ω_j and traversing the obstacles in a 2-periodic manner) and relation (10) is equivalent to

(14)
$$\mathcal{D}\eta^m = f^m, \qquad (m \ge 0),$$

where

$$f^0 = f = 2 (\partial_{\nu} + ik) u^{\text{inc}}, \text{ on } \partial\Omega,$$

and, for $m \geq 1$,

(15)
$$f^m = \begin{bmatrix} 0 & \mathcal{S}_{12} \\ \mathcal{S}_{21} & 0 \end{bmatrix} \eta^{m-1}.$$

In connection with identity (14), Theorem 1 implies in two-dimensional configurations that, given any $k_0 > 0$, there exists $C_{k_0} > 0$ such that for any $k \ge k_0$

(16)
$$\|\eta^{m+2} - \mathcal{R}\eta^m\|_{L^2(\partial\Omega)} \le C_{k_0} \|f^{m+2} - \mathcal{R}f^m\|_{L^2(\partial\Omega)}$$

holds for any constant $\mathcal{R} \in \mathbb{C}$, and thus the aforementioned geometric rate of convergence of the Neumann series (8) is directly linked with that of the right-hand sides f^m . Indeed, assuming that the incidence is a plane-wave $u^{\text{inc}}(x) = e^{ik\alpha \cdot x}$ with direction α ($|\alpha| = 1$) with respect to which the obstacles Ω_1 and Ω_2 satisfy the no-occlusion condition

$$\{x + t\alpha : x \in \partial\Omega_1 \& t \in \mathbb{R}\} \cap \partial\Omega_2 = \emptyset$$

(which amounts to requiring that there is at least one ray with direction α that passes between Ω_1 and Ω_2 without touching them), denoting by $a_j \in \partial \Omega_j$ the uniquely determined points minimizing the distance between Ω_1 and Ω_2 , and setting $d = |a_1 - a_2|$, we have the following relation among the leading terms f_A^m in the asymptotic expansions of f^m which extends our analyses in [20, 5] to the case of CFIE.

THEOREM 3. There exist constants $C = C(\Omega, \alpha) > 0$, $\delta = \delta(\Omega, \alpha) \in (0, 1)$, and $\mathcal{R}_2 = \mathcal{R}_2(\Omega, k) \in \mathbb{C}$ with the property that, for all $m \geq 1$,

(17)
$$\left\| f_A^{m+2} - \mathcal{R}_2 f_A^m \right\|_{L^2(\partial\Omega)} \le C k \, \delta^m.$$

The constant \mathcal{R}_2 is given in two-dimensional configurations by

$$\mathcal{R}_{2} = e^{2ikd} \left(\sqrt{(1+d\kappa_{1})(1+d\kappa_{2})} \times \left[1 + \sqrt{1 - \left[(1+d\kappa_{1})(1+d\kappa_{2}) \right]^{-1}} \right] \right)^{-1},$$

where κ_j is the curvature at the point a_j , and in three-dimensional configurations

$$\mathcal{R}_{2} = e^{2ikd} \left(\sqrt{\det\left[\left(I + d\kappa_{1} \right) \left(I + d\kappa_{2} \right) \right]} \right.$$

$$\times \det\left[I + \sqrt{I - \left[T \left(I + d\kappa_{1} \right) T^{-1} \left(I + d\kappa_{2} \right) \right]^{-1}} \right] \right)^{-1},$$

where I is the identity matrix,

$$\kappa_j = \begin{bmatrix} \kappa_1(a_j) & 0\\ 0 & \kappa_2(a_j) \end{bmatrix}$$

is the matrix of principal curvatures at the point a_j , and T is the rotation matrix determined by the relative orientation of the surfaces $\partial \Omega_j$ at the points a_j .

Proof. Assume first that the dimension is n=2. Writing $f^m=[f_1^m f_2^m]^t$ and $f_A^m=[f_{A,1}^m f_{A,2}^m]^t$, it suffices to show that, for $\ell=1,2$,

(18)
$$\left\| f_{A,\ell}^{(m+2)} - \mathcal{R}_2 f_{A,\ell}^m \right\|_{L^2(\partial\Omega_\ell)} \le C_\ell \, k \, \delta^m$$

for some constant $C_{\ell} = C_{\ell}(\Omega, \alpha)$. On the other hand, [20, Theorems 3.4 and 4.1] displays that (a more general version of) this estimate holds on any compact subset of the *illuminated regions* (see the next section for a precise definition of these regions) when $f_{A,\ell}^{m+2}$ and $f_{A,\ell}^{m}$ are replaced by the leading terms $\eta_{A,\ell}^{m+1}$ and $\eta_{A,\ell}^{m-1}$ in the asymptotic expansions of η_{ℓ}^{m+1} and η_{ℓ}^{m-1} . Finally applying the stationary phase lemma [23] to each component of identity (15), the same techniques used to prove [20, Theorem 4.1] deliver estimate (18). In the case n=3, the argument is the same and is based upon [5, Theorems 3.3 and 4.3].

Although Theorem 3 is valid under the no-occlusion condition, extensive numerical tests in [20, 5] display that the conclusion of Theorem 3 is valid not only when this condition is violated but also when the convexity assumption is conveniently relaxed. For theoretical considerations in the present manuscript, however, we will continue to assume that the obstacles are smooth and strictly convex.

Remark 4. In light of estimates (16)–(17), for $M \gg \log k$, we have

$$\eta = \sum_{m=0}^{\infty} \eta^m \sim \sum_{m=0}^{M} \eta^m + (\eta^{M+1} + \eta^{M+2}) \sum_{m=0}^{\infty} \mathcal{R}_2^m,$$

which signifies that the Neumann series converges with the geometric rate \mathcal{R}_2 . Note however that, as the distance between the obstacles Ω_1 and Ω_2 decreases to zero, $|\mathcal{R}_2|$ increases to 1, and thus convergence of the Neumann series significantly deteriorates.

The same remark is valid when the configuration consists of more than two subscatterers and involves at least one pair of nearby obstacles. Indeed, as we have shown in [20, 5], this is also completely transparent from a theoretical point of view since, in this case, the Neumann series can be completely dismantled into single-scattering effects and rearranged into a sum over *primitive periodic orbits* including, in particular, 2-periodic orbits.

The next section is devoted to the description of how we adopt the high-frequency integral equation method in [14] to the evaluation of iterates arising in our Krylov subspace approach and also in its preconditioning through Kirchhoff approximations. As explained in the introduction, the strength of the work in [14] is due to retaining information on the phases of multiple scattering iterations, and therefore our Krylov subspace and Kirchhoff preconditioning strategies are also designed to posses the same property.

4. High-frequency integral equations for multiple scattering configurations. For simplicity of exposition we continue to assume that the obstacle Ω consists only of two disjoint subscatterers Ω_1 and Ω_2 . In what follows, for $j, j' \in \{1, 2\}$, we will always assume that $j \neq j'$. In this case, relation (14) can be written, for j = 1, 2, in components as

(19)
$$(\mathcal{I} - \mathcal{S}_{jj}) \eta_j^0 = f_j^0 \quad \text{on } \partial \Omega_j$$

and

(20)
$$(\mathcal{I} - \mathcal{S}_{jj}) \eta_i^m = \mathcal{S}_{jj'} \eta_{i'}^{m-1} \quad \text{on } \partial \Omega_j$$

for $m \geq 1$. As identity (19) displays, η_j^0 is exactly the surface current generated by the incidence $u^{\rm inc}$ on $\partial\Omega_j$ ignoring interactions between Ω_1 and Ω_2 . Similarly, for $m \geq 1$, (20) depicts that η_j^m is precisely the surface current generated by the field $u_{j'}^{m-1}$ (note that $\mathcal{S}_{jj'}$ $\eta_{j'}^{m-1} = 2 \left(\partial_{\nu} + ik \right) u_{j'}^{m-1} \right)$ acting as an incidence on $\partial\Omega_j$ ignoring, again, interactions between Ω_1 and Ω_2 . Therefore identities (19) and (20) entail that the Neumann series (8) completely dismantles the single scattering contributions and allows for a representation of the surface current η as a superposition of these effects. More importantly, in geometrically relevant configurations, these observations allow us to predetermine the phase φ_j^m of η_j^m and express it as the product of a highly oscillating complex exponential modulated by a slowly varying amplitude in the form

(21)
$$\eta_j^m = e^{ik\,\varphi_j^m} \,\, \eta_j^{m,\,\text{slow}}$$

and this, in turn, grants the frequency-independent solution of (19)–(20) as described in [14]. To review the algorithm in [14] and set the stage for the rest of the paper, we first describe the phase functions φ_j^m in combination with the various regions they determine on the boundary of the scatterers, and we present one of the main results in [20, 5] that displays the asymptotic characteristics of the amplitudes $\eta_i^{m, \text{slow}}$.

Indeed, in the case the obstacles Ω_1 and Ω_2 are smooth, strictly convex, and satisfy the no-occlusion condition with respect to the direction of incidence α , the phase φ_j^m in (21) is given by

(22)
$$\varphi_1^m = \begin{cases} \phi_1^m, & m \text{ is even,} \\ \phi_2^m, & m \text{ is odd,} \end{cases} \quad \text{and} \quad \varphi_2^m = \begin{cases} \phi_2^m, & m \text{ is even,} \\ \phi_1^m, & m \text{ is odd.} \end{cases}$$

Here, for any of the two obstacle paths $\{\Gamma_1^m\}_{m\geq 0}$ and $\{\Gamma_2^m\}_{m\geq 0}$ defined by

$$\left(\Gamma_1^{2m},\Gamma_1^{2m+1}\right)=\left(\partial\Omega_1,\partial\Omega_2\right)\qquad\text{and}\qquad \left(\Gamma_2^{2m},\Gamma_2^{2m+1}\right)=\left(\partial\Omega_2,\partial\Omega_1\right)$$

for all $m \geq 0$, the geometrical phase ϕ_{ℓ}^m at any point $x \in \Gamma_{\ell}^m$ $(\ell = 1, 2)$ is uniquely defined as [20, 5]

$$\phi_{\ell}^{m}(x) = \begin{cases} \alpha \cdot x, & m = 0, \\ \alpha \cdot \mathcal{X}_{0}^{m}(x) + \sum_{r=0}^{m-1} |\mathcal{X}_{r+1}^{m}(x) - \mathcal{X}_{r}^{m}(x)|, & m \ge 1, \end{cases}$$

where the points $(\mathcal{X}_0^m(x), \dots, \mathcal{X}_m^m(x)) \in \Gamma_\ell^0 \times \dots \times \Gamma_\ell^m$ are specified by

- (a) $\mathcal{X}_m^m(x) = x$,
- (b) $\alpha \cdot \nu(\mathcal{X}_0^m(x)) < 0$,
- (c) $(\mathcal{X}_{r+1}^m(x) \mathcal{X}_r^m(x)) \cdot \nu(\mathcal{X}_r^m(x)) > 0$,

$$(\mathrm{d})\ \frac{\mathcal{X}_1^m(x)-\mathcal{X}_0^m(x)}{|\mathcal{X}_1^m(x)-\mathcal{X}_0^m(x)|}=\alpha-2\alpha\cdot\nu(\mathcal{X}_0^m(x))\,\nu(\mathcal{X}_0^m(x)),$$

(e)
$$\frac{\mathcal{X}_{r+1}^{m}(x) - \mathcal{X}_{r}^{m}(x)}{|\mathcal{X}_{r+1}^{m}(x) - \mathcal{X}_{r}^{m}(x)|} = \frac{\mathcal{X}_{r}^{m}(x) - \mathcal{X}_{r-1}^{m}(x)}{|\mathcal{X}_{r}^{m}(x) - \mathcal{X}_{r-1}^{m}(x)|} - 2\frac{\mathcal{X}_{r}^{m}(x) - \mathcal{X}_{r-1}^{m}(x)}{|\mathcal{X}_{r}^{m}(x) - \mathcal{X}_{r-1}^{m}(x)|} \cdot \nu(\mathcal{X}_{r}^{m}(x)) \nu(\mathcal{X}_{r}^{m}(x))$$

for 0 < r < m. These conditions simply mean the phase $\phi_\ell^m(x)$ is determined by the ray with initial direction α sequentially hitting at and bouncing off the points $\mathcal{X}_r^m(x)$ $(r=0,\ldots,m-1)$ according to the law of reflection to finally arrive at $x \in \Gamma_\ell^m$. Moreover, these rays divide Γ_ℓ^m into two open connected subsets, namely, the illuminated regions

$$\Gamma_\ell^m(IL) = \left\{ \begin{array}{ll} \left\{ x \in \Gamma_\ell^0 : \alpha \cdot \nu(x) < 0 \right\}, & m = 0, \\ \\ \left\{ x \in \Gamma_\ell^m : \left(\mathcal{X}_m^m(x) - \mathcal{X}_{m-1}^m(x) \right) \cdot \nu(x) < 0 \right\}, & m \geq 1, \end{array} \right.$$

and the *shadow regions*

$$\Gamma_{\ell}^{m}(SR) = \left\{ \begin{array}{ll} \left\{ x \in \Gamma_{\ell}^{0} : \alpha \cdot \nu(x) > 0 \right\}, & m = 0, \\ \\ \left\{ x \in \Gamma_{\ell}^{m} : \left(\mathcal{X}_{m}^{m}(x) - \mathcal{X}_{m-1}^{m}(x) \right) \cdot \nu(x) > 0 \right\}, & m \geq 1, \end{array} \right.$$

and their closures intersect at the shadow boundaries

$$\Gamma_{\ell}^{m}(SB) = \left\{ \begin{array}{ll} \left\{ x \in \Gamma_{\ell}^{0} : \alpha \cdot \nu(x) = 0 \right\}, & m = 0, \\ \\ \left\{ x \in \Gamma_{\ell}^{m} : \left(\mathcal{X}_{m}^{m}(x) - \mathcal{X}_{m-1}^{m}(x) \right) \cdot \nu(x) = 0 \right\}, & m \geq 1, \end{array} \right.$$

each of which consists of two points in two-dimensional configurations or a smooth closed curve in three dimensions. In connection with the phase functions (22), illuminated regions $\partial \Omega_j^m(IL)$, shadow regions $\partial \Omega_j^m(SR)$, and the shadow boundaries $\partial \Omega_j^m(SR)$ are then given by

$$\partial\Omega_1^m(\,\cdot\,) = \left\{ \begin{array}{ll} \Gamma_1^m(\,\cdot\,), & m \text{ is even,} \\ \Gamma_2^m(\,\cdot\,), & m \text{ is odd,} \end{array} \right. \quad \text{and} \quad \partial\Omega_2^m(\,\cdot\,) = \left\{ \begin{array}{ll} \Gamma_2^m(\,\cdot\,), & m \text{ is even,} \\ \Gamma_1^m(\,\cdot\,), & m \text{ is odd.} \end{array} \right.$$

Generally speaking this means that the rays emanating from $\partial \Omega_j^m$ return to $\partial \Omega_j^m$ after an even number of reflections, and those initiating from $\partial \Omega_j^m$ arrive $\partial \Omega_j^m$ after an odd number of reflections. Finally let us note that the phase functions ϕ_j^m are smooth and periodic as they are confined to the boundary of the associated scatterers. The computation of these phases are performed using a spectrally accurate geometrical optics solver. This also allows for a simple and accurate determination of the shadow boundary points and thus the illuminated and shadow regions.

With these definitions we can now state one of the main results in [20, 5] that completely clarifies the asymptotic behavior of amplitudes $\eta_i^{m, \text{slow}}$ in (21).

THEOREM 5 (see [20, 5]).

(i) On the illuminated region $\partial \Omega_j^m(IL)$, $\eta_j^{m, \text{slow}}(x, k)$ belongs to the Hörmander class $S_{1,0}^1(\partial \Omega_j^m(IL) \times (0, \infty))$ (cf. [30, 31]) and admits the asymptotic expansion

(23)
$$\eta_j^{m, \text{slow}}(x, k) \sim \sum_{p \ge 0} k^{1-p} a_{j,p}^m(x),$$

where $a_{j,p}^m$ are complex-valued C^{∞} functions. Consequently, for any $P \in \mathbb{N} \cup \{0\}$, the difference

(24)
$$r_{j,P}^{m}(x,k) = \eta_{j}^{m,\text{slow}}(x,k) - \sum_{p=0}^{P} k^{1-p} a_{j,p}^{m}(x)$$

belongs to $S_{1,0}^{-P}(\partial \Omega_j^m(IL) \times (0,\infty))$ and thus satisfies the estimates

(25)
$$|D_x^{\beta} D_k^n r_{j,N}^m(x,k)| \le C_{m,\beta,n,S} (1+k)^{-P-n}$$

on any compact subset S of $\partial\Omega_j^m(IL)$ for any multi-index β and $n\in\mathbb{N}\cup\{0\}$.

(ii) Over the entire boundary $\partial\Omega_j$, $\eta_j^{m, \text{slow}}(x, k)$ belongs to the Hörmander class $S^1_{2/3,1/3}(\partial\Omega_j\times(0,\infty))$ and admits the asymptotic expansion

(26)
$$\eta_j^{m, \text{slow}}(x, k) \sim \sum_{p,q \ge 0} k^{2/3 - 2p/3 - q} b_{j,p,q}^m(x) \Psi^{(p)}(k^{1/3} Z_j^m(x)),$$

where $b^m_{j,p,q}(x)$ are complex-valued C^{∞} functions, $Z^m_j(x)$ is a real-valued C^{∞} function that is positive on $\partial \Omega^m_j(IL)$, negative on $\partial \Omega^m_j(SR)$, and vanishes precisely to first order on $\partial \Omega^m_j(SB)$, and the function Ψ admits the asymptotic expansion

(27)
$$\Psi(\tau) \sim \sum_{\ell > 0} c_{\ell} \tau^{1-3\ell} \quad as \ \tau \to \infty,$$

and it is rapidly decreasing in the sense of Schwartz as $\tau \to -\infty$. Note specifically then, for any $P, Q \in \mathbb{N} \cup \{0\}$, the difference

$$R_{P,Q}^m(x,k) = \eta_j^{m,\text{slow}}(x,k) - \sum_{p,q=0}^{P,Q} k^{2/3 - 2p/3 - q} b_{j,p,q}^m(x) \Psi^{(p)}(k^{1/3} Z_j^m(x))$$

belongs to $S_{2/3,1/3}^{-\mu}(\partial\Omega_j\times(0,\infty))$, $\mu=\min\{2P/3,Q\}$, and thus satisfies the estimates

(28)
$$|D_x^{\beta} D_k^n R_{P,Q}^m(x,k)| \le C_{m,\beta,n} (1+k)^{-\mu-2n/3+|\beta|/3}$$

for any multi-index β and $n \in \mathbb{N} \cup \{0\}$.

The first main ingredient underlying the algorithm in [14] was the observation that, while $\eta_j^{m, \text{slow}}$ admits a classical asymptotic expansion in the illuminated region $\partial \Omega_j^m(IL)$ as displayed by (23), it possesses boundary layers of order $\mathcal{O}(k^{-1/3})$ around the shadow boundaries $\partial \Omega_j^m(SB)$ and rapidly decays in the shadow region $\partial \Omega_j^m(SR)$ as implied by the expansion (26) and the mentioned change in the asymptotic expansions of the function Ψ . Therefore, as depicted in [14], utilizing a cubic root change of variables in k around the shadow boundaries, the unknown $\eta_j^{m, \text{slow}}$ can be expressed in a number of degrees of freedom independent of frequency, and this transforms the problem into the evaluation of highly oscillatory integrals.

Indeed, a second main element of the algorithm in [14] is based on the realization that the identity

(29)
$$\frac{d}{dz}H_0^{(1)}(z) = -H_1^{(1)}(z)$$

combined with the asymptotic expansions of Hankel functions [3] entails

$$\left(\partial_{\nu(x)} + ik\right)G(x,y) \sim e^{ik|x-y|} \left(e^{-i\pi/4} \left(\frac{k}{2\pi|x-y|}\right)^{1/2} \left(1 + \frac{x-y}{|x-y|} \cdot \nu(x)\right)\right),$$

and thus, in light of factorization (21), (19)–(20) take on the form (30)

$$e^{ik\,\varphi_j^0(x)}\,\,\eta_j^{0,\,\mathrm{slow}}(x) - \int_{\partial\Omega_j} e^{ik\,(\varphi_j^0(y) + |x-y|)}\,F(x,y)\,\,\eta_j^{0,\,\mathrm{slow}}(y)\,ds(y) = f_j^0(x),\quad x\in\partial\Omega_j^0,$$

and, for $m \geq 1$,

$$(31) \quad e^{ik\,\varphi_j^m(x)} \,\, \eta_j^{m,\,\mathrm{slow}}(x) - \int_{\partial\Omega_j} e^{ik\,(\varphi_j^m(y) + |x-y|)} \,F(x,y) \,\eta_j^{m,\,\mathrm{slow}}(y) \,ds(y)$$

$$= \int_{\partial\Omega_{s'}} e^{ik\,(\varphi_j^{m-1}(y) + |x-y|)} \,F(x,y) \,\eta_{j'}^{m-1,\,\mathrm{slow}}(y) \,ds(y), \quad x \in \partial\Omega_j^m,$$

where

$$F(x,y) = e^{-ik|x-y|} \left(\partial_{\nu(x)} + ik \right) G(x,y).$$

As depicted in [14], frequency independent evaluations of integrals in (30)–(31) can then be accomplished to any desired accuracy utilizing a localized integration (around stationary points of the combined phase $\varphi_j^m(y) + |x - y|$ or the singularities of the integrand) procedure based upon suitable extensions of the method of stationary phase.

The third main element of the algorithm in [14] is the use of Nysröm and trapezoidal discretizations and Fourier interpolations to render the method high order, and the scheme is finally completed with a matrix-free Krylov subspace linear algebra solver to obtain accelerated solutions.

While the above discussion provides a brief summary of the algorithm in [14], it clearly signifies the importance of retaining the phase information in connection with the multiple scattering iterations since this allows for a simple utilization of the aforementioned localized integration scheme. Accordingly, any strategy aiming at accelerating the convergence of Neumann series must also preserve the phase information. As we explain, both the novel Krylov subspace method we develop in the next section and its preconditioning discussed in section 6 possess this property.

5. Novel Krylov subspace method for accelerating the convergence of Neumann series. As with the solution of matrix equations, Krylov subspace methods provide a convenient mechanism for the approximate solution of operator equations

$$\mathcal{A}\eta = g$$

in Hilbert spaces (see, e.g., [34] and the references therein). These methods are orthogonal projection methods wherein, given an initial approximation $\mu^{(0)}$ to η , one seeks an approximate solution $\mu^{(m)}$ from the affine space $\mu^{(0)} + K_m$ related with the Krylov subspace

$$K_m = \text{span}\left\{r^{(0)}, Ar^{(0)}, A^2r^{(0)}, \dots, A^{m-1}r^{(0)}\right\}$$

of the operator \mathcal{A} associated with the residual $r^{(0)} = g - \mathcal{A}\mu^{(0)}$ imposing the Petrov-Galerkin condition

$$g - \mathcal{A}\mu^{(m)} \perp K_m$$
.

In connection with the operator equation (6), taking $\mathcal{A} = \mathcal{I} - \mathcal{T}$ and $\mu^{(0)} = 0$, the approximate solution $\mu^{(m)}$ belongs to the Krylov subspace

$$K_m = \operatorname{span} \left\{ g, (\mathcal{I} - \mathcal{T})g, (\mathcal{I} - \mathcal{T})^2 g, \dots, (\mathcal{I} - \mathcal{T})^{m-1} g \right\}$$

for which, in light of identity (10), the functions $(\mathcal{I} - \mathcal{T})^n g$ can be expressed as linear combinations of the multiple scattering iterations η^{ℓ} through use of the binomial theorem as

(32)
$$(\mathcal{I} - \mathcal{T})^n g = \sum_{\ell=0}^n \binom{n}{\ell} (-1)^{\ell} \mathcal{T}^{\ell} g = \sum_{\ell=0}^n \binom{n}{\ell} (-1)^{\ell} \eta^{\ell}.$$

This relation clearly entails

$$K_m = \operatorname{span}\left\{\eta^0, \dots, \eta^{m-1}\right\}$$

and thus, any information about the Krylov subspace K_m can be obtained in frequency independent computational times using the algorithm briefly described in section 4.

A particular Krylov subspace method we favor for the solution of multiple scattering problem (6) is the classical ORTHODIR [34] iteration which, for the initial guess $\mu^{(0)} = 0$, takes on the form

1. Set
$$r^{(0)} = p^{(0)} = g$$
,
2. For $j = 0, 1 ...$ DO
2.1 $\alpha_j = \langle r^{(j)}, \mathcal{A}p^{(j)} \rangle / \langle \mathcal{A}p^{(j)}, \mathcal{A}p^{(j)} \rangle$,
2.2 $\mu^{(j+1)} = \mu^{(j)} + \alpha_j p^{(j)}$,
2.3 $r^{(j+1)} = r^{(j)} - \alpha_j \mathcal{A}p^{(j)}$,
2.4 For $i = 0, ..., j$, $\beta_{ij} = -\langle \mathcal{A}^2 p^{(j)}, \mathcal{A}p^{(i)} \rangle / \langle \mathcal{A}p^{(i)}, \mathcal{A}p^{(i)} \rangle$,
2.5 $p^{(j+1)} = \mathcal{A}p^{(j)} + \sum_{i=0}^{j} \beta_{ij} p^{(i)}$.

This iteration entails, through a straightforward induction argument, the following recurrence relation for $\mathcal{A} = \mathcal{I} - \mathcal{T}$, where \mathcal{T} is the iteration operator specified by (7).

Theorem 6. For A = I - T, the iterates $p^{(j)}$ generated by the ORTHODIR algorithm satisfy the recurrence relation

(33)
$$p^{(j)} = (\mathcal{I} - \mathcal{T})^j p^{(0)} + \sum_{\ell=0}^{j-1} \sum_{i=0}^{\ell} \beta_{i\ell} (\mathcal{I} - \mathcal{T})^{j-1-\ell} p^{(i)}, \qquad j = 0, 1, \dots$$

Although this relation can be used in combination with the binomial identity (32) to recursively compute $p^{(j)}$, this approach is bound to result in numerical instabilities when the distance d between the obstacles Ω_1 and Ω_2 is close to zero since, in this case, the asymptotic rate of convergence \mathcal{R}_2 is close to 1. Concentrating, for instance, on the term $(\mathcal{I} - \mathcal{T})^j p^{(0)}$, this instability is apparent from the subtractive cancellations in binomial identity (32) upon noting that $p^{(0)} = g$ and $\eta^{\ell+2} \sim \mathcal{R}_2 \eta^{\ell} \sim \eta^{\ell}$ for $\ell \gg \log k$ by inequality (16) and Theorem 3.

On the other hand, since $p^{(0)} = g$, a combined use of (32) and (33) clearly shows that the iterates $p^{(j)}$ generated by the ORTHODIR algorithms can alternatively be computed through the following *identification procedure*.

COROLLARY 7. Each $p^{(j)}$ is a linear combination of η^0, \ldots, η^j , say,

(34)
$$p^{(j)} = \sum_{i=0}^{j} \gamma_{ij} \, \eta^{i},$$

and this allows for the computation of the next iterate as

$$p^{(j+1)} = (\mathcal{I} - \mathcal{T}) p^{(j)} + \sum_{i=0}^{j} \beta_{ij} p^{(i)} = \sum_{i=0}^{j} \gamma_{ij} \eta^{i} - \sum_{i=0}^{j} \gamma_{ij} \eta^{i+1} + \sum_{i=0}^{j} \beta_{ij} p^{(i)}$$

$$= \sum_{i=0}^{j+1} \gamma_{i,j+1} \eta^{i},$$
(35)

where the new coefficients $\gamma_{i,j+1}$ are easily computed by identification.

In connection with step 2 in the ORTHODIR iteration we note explicitly that

$$\mathcal{T}p^{(j)} = \sum_{i=0}^{j} \gamma_{ij} \, \eta^{i+1}$$
 and $\mathcal{T}^2 p^{(j)} = \sum_{i=0}^{j} \gamma_{ij} \, \eta^{i+2}$

and these can then be used to easily evaluate $\mathcal{A}p^{(j)} = (\mathcal{I} - \mathcal{T})p^{(j)}$ and $\mathcal{A}^2p^{(j)} = (\mathcal{I} - 2\mathcal{T} + \mathcal{T}^2)p^{(j)}$. Let us mention that in the evaluation of $\mathcal{A}^2p^{(j)}$, we only need to compute the quantity $\mathcal{T}^2p^{(j)}$ because the one related to $(I - 2\mathcal{T})p^{(j)}$ is derived from the previous calculations in the same iteration. As for the identification procedure, we have

$$p^{(j+1)} = \mathcal{A}p^{(j)} + \sum_{i=0}^{j} \beta_{ij} p^{(i)} = \sum_{i=0}^{j} \gamma_{ij} \eta^{i} - \sum_{i=0}^{j} \gamma_{ij} \eta^{i+1} + \sum_{i=0}^{j} \beta_{ij} \sum_{\ell=0}^{i} \gamma_{\ell i} \eta^{\ell}$$

so that interchanging the order of summation in the double sum in this latter identity,

we obtain the explicit expression

$$p^{(j+1)} = \sum_{i=0}^{j} \gamma_{ij} \, \eta^{i} - \sum_{i=0}^{j} \gamma_{i,j} \, \eta^{i+1} + \sum_{i=0}^{j} \sum_{\ell=i}^{j} \beta_{\ell j} \, \gamma_{i\ell} \, \eta^{i}$$

$$= \left(\gamma_{0j} + \sum_{\ell=0}^{j} \beta_{\ell j} \, \gamma_{0\ell} \right) \eta^{0} + \sum_{i=1}^{j} \left(\gamma_{ij} - \gamma_{i-1,j} + \sum_{\ell=i}^{j} \beta_{\ell j} \, \gamma_{i\ell} \right) \eta^{i} - \gamma_{jj} \, \eta^{j+1}$$

$$= \sum_{i=0}^{j+1} \gamma_{i,j+1} \, \eta^{i}.$$

In light of these identities, we note specifically that since the phases of η^i are known, identity (34) allows for a utilization of the *localized integration* scheme briefly summarized in section 4 in the evaluation of inner products in steps 2.1 and 2.4 in the ORTHODIR iteration. On the other hand, the identification procedure (35) provides a numerically stable way of recursively computing $p^{(j)}$ as it clearly eliminates subtractive cancellations arising from the use of binomial identity (32).

6. Preconditioning using Kirchhoff approximations. Although the novel Krylov subspace approach discussed in the previous section provides an effective mechanism for the accelerated solution of multiple scattering problem (6), this can be further improved if the operator equation (6) is properly preconditioned. Indeed, for an appropriately defined operator \mathcal{K} approximating the iteration operator \mathcal{T} , the preconditioned form of (6) reads

(36)
$$(\mathcal{I} - \mathcal{K})^{-1} (\mathcal{I} - \mathcal{T}) \eta = (\mathcal{I} - \mathcal{K})^{-1} g.$$

In this connection, we note the following useful alternative.

THEOREM 8. If the spectral radius r(K) of K is strictly less than 1, then the preconditioned equation (36) can be written alternatively as

(37)
$$\left(\mathcal{I} - \sum_{\ell=0}^{\infty} \mathcal{K}^{\ell} \left(\mathcal{T} - \mathcal{K} \right) \right) \eta = \sum_{\ell=0}^{\infty} \mathcal{K}^{\ell} g.$$

Proof. Since $r(\mathcal{K}) < 1$, we have the Neumann series representation [33]

(38)
$$(\mathcal{I} - \mathcal{K})^{-1} = \sum_{\ell=0}^{\infty} \mathcal{K}^{\ell}.$$

Use of (38) in the identity

$$\left(\mathcal{I}-\mathcal{K}\right)^{-1}\left(\mathcal{I}-\mathcal{T}\right)=\mathcal{I}-\left(\mathcal{I}-\mathcal{K}\right)^{-1}\left(\mathcal{T}-\mathcal{K}\right)$$

delivers the desired result.

It is therefore natural to approximate the solution of (6) with the solution of the truncated equation

(39)
$$\left(\mathcal{I} - \sum_{\ell=0}^{N} \mathcal{K}^{\ell} \left(\mathcal{T} - \mathcal{K} \right) \right) \eta = \sum_{\ell=0}^{M} \mathcal{K}^{\ell} g,$$

which we shall write as

$$\mathcal{A}_{\kappa,N} \eta = g_{\kappa,M}.$$

While (40) displays the preconditioning strategy we shall utilize for the solution of multiple scattering problem (6), it is clearly amenable to a treatment by the Krylov subspace method developed in the preceding section to further accelerate the solution of problem (6).

As for the requirement that K has to approximate the iteration operator \mathcal{T} , we recall that each application of \mathcal{T} corresponds exactly to the evaluation of the surface current on each of the obstacles Ω_1 and Ω_2 generated by the fields scattered from, respectively, Ω_2 and Ω_1 at the previous reflection as depicted by the identity

$$\begin{bmatrix} \eta_1^m \\ \eta_2^m \end{bmatrix} = \mathcal{T} \begin{bmatrix} \eta_1^{m-1} \\ \eta_2^{m-1} \end{bmatrix} = \begin{bmatrix} 0 & (\mathcal{I} - \mathcal{S}_{11})^{-1} \mathcal{S}_{12} \\ (\mathcal{I} - \mathcal{S}_{22})^{-1} \mathcal{S}_{21} & 0 \end{bmatrix} \begin{bmatrix} \eta_1^{m-1} \\ \eta_2^{m-1} \end{bmatrix}.$$

It is therefore reasonable to define the operator K in the form

$$\mathcal{K} = \begin{bmatrix} 0 & \mathcal{K}_{12} \\ \mathcal{K}_{21} & 0 \end{bmatrix}$$

and require that $\eta_j^m \approx \mathcal{K}_{jj'} \eta_{j'}^{m-1}$. Accordingly, the operators $\mathcal{K}_{jj'}$ must retain the phase information to preserve the frequency independent operation count while, concurrently, providing a reasonable approximation to the slow densities to guarantee an accurate preconditioning. This requirement can be satisfied only if the operators $\mathcal{K}_{jj'}$ are defined in a dynamical manner so as to respect the information associated with the iterates, and this distinguishes our preconditioning strategy from classical approaches where the preconditioners are steady by design. The most natural approach is to design the operators $\mathcal{K}_{jj'}$ so that they yield the classical Kirchhoff approximations as these preserve the phase information exactly and approximate $\eta_j^{m, \text{slow}}$ with the leading term in its asymptotic expansion. Concentrating on two-dimensional settings, in this connection, a basic relation we exploited in [20] was the observation that while, on the one hand, this term coincides with that of twice the normal derivative of $u_{j'}^{m-1}$ in (12) on the illuminated region $\partial \Omega_j^m(IL)$, and on the other hand, identity (29) combined with asymptotic expansions of Hankel functions [3] entails

(41)
$$\partial_{\nu(x)}G(x,y) \sim e^{ik|x-y|} \left(e^{-i\pi/4} \sqrt{\frac{k}{2\pi|x-y|}} \frac{x-y}{|x-y|} \cdot \nu(x) \right)$$

so that use of (41) in (12) yields

$$2 \, \partial_{\nu(x)} u_{j'}^{m-1}(x) \sim \int_{\partial \Omega_{j'}} \sqrt{\frac{k}{2\pi}} \, e^{ik \, (\varphi_{j'}^{m-1}(y) + |x-y|) - i\pi/4} \eta_{j'}^{m-1, \text{slow}}(y) F(x, y) \, ds(y), \ \ x \in \partial \Omega_{j},$$

where

(43)
$$F(x,y) = \frac{1}{\sqrt{|x-y|}} \frac{x-y}{|x-y|} \cdot \nu(x).$$

As for the oscillatory integral in (42), as we have shown in [20], it is treatable through an appropriate use of *stationary phase method* [23] which states that the main contribution to an oscillatory integral comes from the stationary points of the phase.

LEMMA 9 (stationary phase method). Let $\psi \in C^{\infty}[a,b]$ be real valued, and let $h \in C_0^{\infty}[a,b]$. Suppose that t_0 is the only stationary point of ψ in (a,b), $\psi''(t_0) \neq 0$, and $\sigma = \operatorname{sign} \psi''(t_0)$. Then there exists a constant C such that, for all k > 1,

$$\left| \int_a^b e^{ik\psi(t)} \, h(t) \, dt - e^{ik\psi(t_0) + i\pi\sigma/4} \, h(t_0) \sqrt{\frac{2\pi}{k \, |\psi''t_0|}} \, \right| \le C \, k^{-1} \, \|h\|_{C^2[a,b]}.$$

Indeed, it turns out [20] that the combined phase function

$$\varphi_{jj'}^{m}(x,y) = \varphi_{j'}^{m-1}(y) + |x-y|$$

has two stationary points, one in the shadow region $\partial \Omega_{j'}^{m-1}(SR)$ with a contribution of $\mathcal{O}(k^{-n})$ (for all $n \in \mathbb{N}$) due to rapid decay of the amplitude $\eta_{j'}^{m-1, \text{slow}}$, and another one in the illuminated region $\partial \Omega_{j'}^{m-1}(IL)$ given by $y(x) = \mathcal{X}_{m-1}^m(x)$ (at which the combined phase has a positive "second derivative") whose contribution agrees, to leading order, with that given by stationary phase evaluation of the integral in (42). While this discussion clarifies how Kirchhoff operators $\mathcal{K}_{jj'}$ must be designed so that they yield the leading terms in the asymptotic expansions of η_j^m on the illuminated regions $\partial \Omega_j^m(IL)$ at each iteration, the rapid decay of η_j^m in the shadow region $\partial \Omega_j^m(SR)$, in turn, provides the motivation that $\mathcal{K}_{jj'}$ must simply approximate η_j^m by zero in these regions. Being aware of these, we use $\gamma_j(t_j) = (\gamma_j^1(t_j), \gamma_j^2(t_j))$ to denote the arc length parametrezation of $\partial \Omega_j$ (in the counterclockwise orientation) with period L_j (j=1,2) so that, for each $x_j \in \partial \Omega_j$, t_j is the unique point in $[0,L_j)$ with $\gamma_j(t_j) = x_j$, and define the Kirchhoff operators $\mathcal{K}_{jj'}$ as follows.

DEFINITION 10. For a smooth phase $\phi_{j'}: \partial\Omega_{j'} \to \mathbb{R}$ having the property that, for each $x_j \in \partial\Omega_j$, the function $\phi_{jj'}: \partial\Omega_j \times \partial\Omega_{j'} \to \mathbb{R}$ given by

$$\phi_{jj'}(x_j, x_{j'}) = \phi_{j'}(x_{j'}) + |x_j - x_{j'}|$$

has a unique stationary point $y_{j'} = x_{j'}(x_j) \in \partial \Omega_{j'}$ such that $[x_j, y_{j'}] \cap \partial \Omega_{j'} = y_{j'}$, define the transformed phase $\phi_j : \partial \Omega_j \to \mathbb{R}$ by setting

$$\phi_j(x_j) = \phi_{jj'}(x_j, y_{j'}).$$

Assume further that $\phi_{jj'}(t_j, t_{j'}) = \phi_{jj'}(x_j, x_{j'})$ has $\partial^2_{t_{j'}}\phi_{jj'}(t_j, \tau_{j'}) > 0$ at $\tau_{j'} = \gamma_{j'}^{-1}(y_{j'})$ and for a given amplitude $A_{j'}: \partial\Omega_{j'} \to \mathbb{C}$, define the transformed amplitude $A_j: \partial\Omega_j \to \mathbb{C}$ by setting

$$A_{j}(x_{j}) = \begin{cases} B_{j}(x_{j}) & \text{if } [x_{j}, y_{j'}] \cap \partial \Omega_{j} = \{x_{j}\}, \\ 0 & \text{otherwise,} \end{cases}$$

where, with the function F as defined in (43),

$$B_j(x_j) = A_{j'}(y_{j'}) F(x_j, y_{j'}) \left(\partial_{t_{j'}}^2 \phi_{jj'}(t_j, \tau_{j'}) \right)^{-1/2}.$$

Finally, define the Kirchhoff operator $\mathcal{K}_{jj'}$ by setting

(44)
$$\mathcal{K}_{jj'}(\phi_{j'}, A_{j'}) = (\phi_j, A_j).$$

We abbreviate identity (44) as

(45)
$$\mathcal{K}_{jj'}\left(e^{ik\,\phi_{j'}}\,A_{j'}\right) = e^{ik\,\phi_j}\,A_j$$

and extend $\mathcal{K}_{jj'}$ by linearity so that

(46)
$$\mathcal{K}_{jj'} \left(\sum_{\ell=0}^{N} e^{ik \, \phi_{j'}^{\ell}} \, A_{j'}^{\ell} \right) = \sum_{\ell=0}^{N} \mathcal{K}_{jj'} \left(e^{ik \, \phi_{j'}^{\ell}} \, A_{j'}^{\ell} \right).$$

In connection with the requirement that the operators $\mathcal{K}_{jj'}$ must retain the phase information exactly while providing a reasonable approximation to the slow densities, we note that

$$\mathcal{K}_{jj'}\left(e^{ik\,\varphi_{j'}^{m-1}}\,\eta_{j'}^{m-1,\,\mathrm{slow}}\right)(x) = e^{ik\,\varphi_{j}^{m}(x)}\,\lambda_{j}^{m,\,\mathrm{slow}}(x), \quad x \in \partial\Omega_{j},$$

where, with F as given in (43),

$$\begin{split} \lambda_j^{m,\,\mathrm{slow}}(x) \\ &= \left\{ \begin{array}{ll} \eta_{j'}^{m-1,\,\mathrm{slow}}(\mathcal{X}_{m-1}^m(x))\,F(x,\mathcal{X}_{m-1}^m(x))\,(\partial_{t_{j'}}^2\varphi_{jj'}^m(t_j,\tau_{j'}))^{-1/2}, & x \in \partial\Omega_j^m(IL), \\ 0, & \mathrm{otherwise}, \end{array} \right. \end{split}$$

so that $\mathcal{K}_{jj'}$ preserves the phase information, and the leading term in the asymptotic expansion of $\lambda_j^{m, \text{slow}}$ agrees with that of $\eta_j^{m, \text{slow}}$ in the illuminated region $\partial \Omega_j^m(IL)$ as desired (cf. [20, Theorems 3.3 and 3.4]).

As for the alternative form (37) of the preconditioned equation (36), we have the following result.

THEOREM 11. Suppose that the obstacles Ω_1 and Ω_2 satisfy the no-occlusion condition with respect to the direction of incidence α . Considering any given function $h \in C(\partial\Omega)$ as $h(x) = e^{ik \cdot \alpha \cdot x} h_0(x)$, the series

$$\sum_{\ell=0}^{\infty} \|\mathcal{K}^{\ell} h\|_{\infty}$$

converges for all k > 0.

Proof. The same technique used to prove [20, Theorem 4.1] entails the existence of constants $C = C(\Omega, \alpha) > 0$ and $\delta = \delta(\Omega, \alpha) \in (0, 1)$ such that, for all $\ell \in \mathbb{Z}_+$,

$$\left\|\mathcal{K}^{\ell+2}h - \mathcal{R}_2 \mathcal{K}^{\ell} h\right\|_{\infty} \leq \delta^{\ell} \left(\min\left\{2, \exp\left(Ck \, \delta^{\ell}\right) - 1\right\} \delta^2 + C \delta^{\ell-2}\right) \|h\|_{\infty},$$

which yields

$$\left\|\mathcal{K}^{\ell+2}h - \mathcal{R}_2\mathcal{K}^{\ell}h\right\|_{\infty} \leq \delta^{\ell} \left(2\delta^2 + C\delta^{\ell-2}\right) \|h\|_{\infty}.$$

Using $C = C(\Omega, \alpha)$ to denote a positive constant whose value may be different at each appearance in what follows, this inequality clearly implies

$$\|\mathcal{K}^{\ell+2}h - \mathcal{R}_2\mathcal{K}^{\ell}h\|_{\infty} \le C \delta^{\ell}\|h\|_{\infty}.$$

Since $|\mathcal{R}_2| < 1$, choosing δ larger, if necessary, we may assume that $\delta^2 \in (|\mathcal{R}_2|, 1)$. In this case, the preceding inequality yields, for $\ell \in \mathbb{Z}_+$ and m = 0, 1,

$$\begin{split} \left\| \mathcal{K}^{m+2\ell} h \right\|_{\infty} & \leq \left\| \mathcal{R}_{2}^{\ell} \, \mathcal{K}^{m} h \right\|_{\infty} + \sum_{j=0}^{\ell-1} \left\| \mathcal{R}_{2}^{\ell-(j+1)} \mathcal{K}^{m+2(j+1)} h - \mathcal{R}_{2}^{\ell-j} \mathcal{K}^{m+2j} h \right\|_{\infty} \\ & = |\mathcal{R}_{2}|^{\ell} \, \| \mathcal{K}^{m} h \|_{\infty} + \sum_{j=0}^{\ell-1} |\mathcal{R}_{2}|^{\ell-(j+1)} \, \left\| \mathcal{K}^{m+2(j+1)} h - \mathcal{R}_{2} \mathcal{K}^{m+2j} h \right\|_{\infty} \\ & \leq |\mathcal{R}_{2}|^{\ell} \, \| \mathcal{K}^{m} h \|_{\infty} + C \sum_{j=0}^{\ell-1} |\mathcal{R}_{2}|^{\ell-(j+1)} \delta^{m+2j} \| h \|_{\infty} \\ & = |\mathcal{R}_{2}|^{\ell} \, \| \mathcal{K}^{m} h \|_{\infty} + C \, \delta^{m} \frac{|\mathcal{R}_{2}|^{\ell} - \delta^{2\ell}}{|\mathcal{R}_{2}| - \delta^{2}} \| h \|_{\infty} \\ & \leq \delta^{2\ell} \, \| \mathcal{K}^{m} h \|_{\infty} + C \, \delta^{m+2\ell} \| h \|_{\infty}. \end{split}$$

Since we clearly have $\|\mathcal{K}^m h\|_{\infty} \leq C\|h\|_{\infty}$ for m = 0, 1, we conclude

$$\left\|\mathcal{K}^{m+2\ell}h\right\|_{\infty} \leq C\left(\delta^{2\ell} + \delta^{m+2\ell}\right)\|h\|_{\infty} \leq C\,\delta^{m+2\ell}\,\|h\|_{\infty},$$

and this gives, for all $\ell \in \mathbb{Z}_+$,

$$\left\| \mathcal{K}^{\ell} h \right\|_{\infty} \leq C \, \delta^{\ell} \, \|h\|_{\infty}.$$

Thus the result follows

Remark 12. Considering K as an operator $K: C(\partial\Omega) \to C(\partial\Omega)$, inequality (47) implies

$$r(\mathcal{K}) = \lim_{\ell \to \infty} \|\mathcal{K}^{\ell}\|_{\infty}^{1/\ell} \le \delta < 1$$

for the spectral radius of K, and this explains the sense in which identity (37) in Theorem 8 holds.

In connection with the application of the ORTHODIR iteration to the preconditioned equation (39), setting $\varphi^m = [\varphi_1^m, \varphi_2^m]^t$ and using μ^ℓ ($\ell = 0, 1, ...$) to denote generic functions defined on $\partial\Omega$ which may be different from line to line, we thus see through (45)–(46) that

$$p^{(0)} = g_{\kappa,M} = \sum_{\ell=0}^{N} \mathcal{K}^{\ell} g = \sum_{\ell=0}^{M} \mathcal{K}^{\ell} \left(e^{ik \varphi^{0}} \eta^{0, \text{slow}} \right)$$

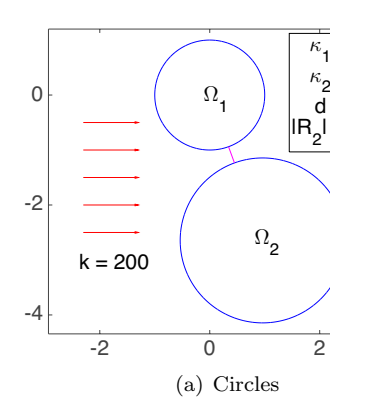
is of the form

(48)
$$p^{(0)} = \sum_{\ell=0}^{M} e^{ik \, \varphi^{\ell}} \mu^{\ell}.$$

More generally, we have the following result.

THEOREM 13. For j = 0, 1, 2..., the ORTHODIR iterates $p^{(j)}$ are of the form

(49)
$$p^{(j)} = \sum_{\ell=0}^{M+j(N+1)} e^{ik\,\varphi^{\ell}} \mu^{\ell}.$$



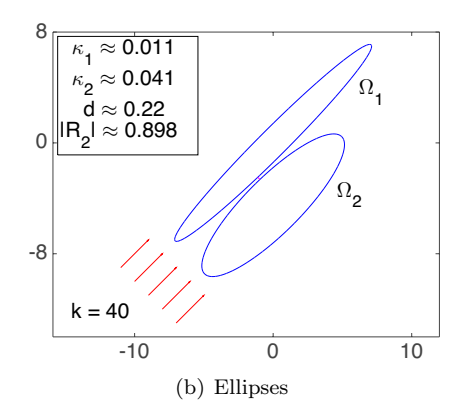


Fig. 1. Multiple scattering configurations.

Proof. This follows by a straightforward induction based on (45)–(46), (48), and the recursion

$$(50) p^{(j+1)} = \mathcal{A}_{\kappa,N} p^{(j)} + \sum_{i=0}^{j} \beta_{ij} p^{(i)} = \left(\mathcal{I} - \sum_{\ell=0}^{N} \mathcal{K}^{\ell} \left(\mathcal{T} - \mathcal{K} \right) \right) p^{(j)} + \sum_{i=0}^{j} \beta_{ij} p^{(i)}.$$

The main point behind this theorem is that use of (49) in (50) clearly allows for an application of the aforementioned localized integration scheme in connection with the execution of the operator \mathcal{T} in (50). Moreover, it is clear that each realization of the Kirchhoff operator \mathcal{K} is frequency independent. Consequently, the preconditioned equation (39) is amenable to a treatment by the Krylov subspace method described in section 5 to obtain even more accelerated solutions of the multiple scattering problem (6) while still retaining the frequency independent operation count if desired.

7. Numerical implementations. In this section we present several numerical examples that display the benefits of our Krylov subspace approach as well as its preconditioning based on the Kirchhoff approximations. The results are produced on a single core (3.7 GHz Intel Xeon processor) of a MacPro machine with 64Gb of memory by a MATLAB implementation of our algorithm. In all the examples, we use the high frequency integral equations (30) and (31) or their generalized versions as described in [20]. For implementation details regarding the frequency independent numerical solution of these integral equations we refer to [13].

The first two examples concern two smooth convex obstacles consisting of circles and ellipses (see Figure 1). The radii of the circles are 1 and 1.5, they are centered at the origin and (0.9625, -2.6444), and they are illuminated by a plane-wave incidence coming in from the left with wavenumber k = 200. Ellipses are chosen to be parallel with centers at (0,0) and (0,-4.5) and major/minor axes 10/1 and 7/2. In this case the illumination is provided by a plane wave with direction along the major axes and wavenumber k = 40. For both configurations, the number of points we have used to discretize the high frequency integral equations (30) and (31) on the surface of each scatterer is 240.

Figure 2 provides a comparison of (a) the Neumann series, (b) the Padé approximants, (c) the Krylov subspace method based on a combined use of binomial formula (32) and identity (33), and (d) the alternative implementation of the latter based on decomposition (34) leading to (35). More precisely, Figure 2 depicts the number of

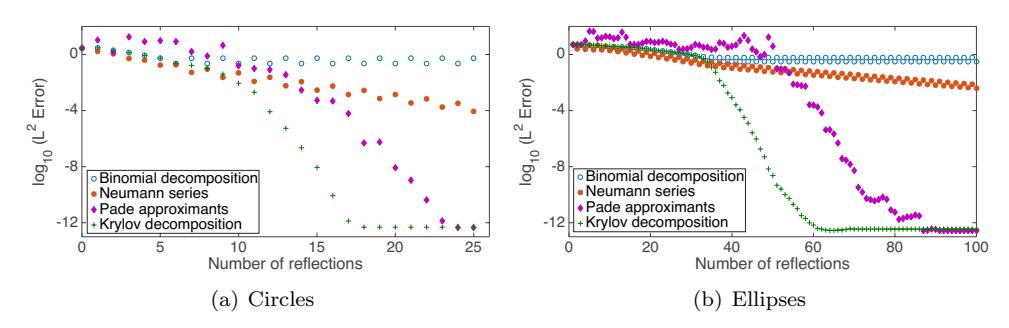


Fig. 2. Acceleration provided by the Krylov subspace method.

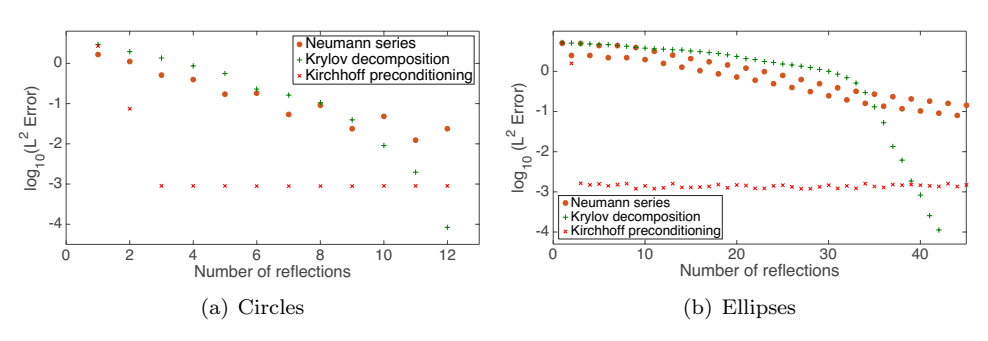


Fig. 3. Preconditioning through Kirchhoff approximations.

reflections versus the logarithmic L^2 error

$$\log_{10} \|\eta - \hat{\eta}\|_2$$

between the exact solution η and the approximations $\hat{\eta}$ obtained by the four aforementioned schemes. In both cases, the reference solution η is computed using an integral solver with sufficiently many disretization points to guarantee 14 digits of accuracy. As we anticipated, combined use of binomial formula (32) and identity (33) suffers from subtractive cancellations and fails to approximate the solution as the number of reflections increases. The implementation of the Krylov subspace method based on decomposition (34) and the resulting equation (35) clearly resolves this issue. Furthermore, when compared with the Padé approximants considered in [14], approximations provided by this alternative implementation of the Krylov subspace method are more stable and give better accuracy at each iteration. Incidentally, note specifically that a direct use of Neumann series would require about 77/522 iterations to obtain 12 digits of accuracy for circular/elliptical configurations in Figure 1, and thus our Krylov subspace approach provides savings of 78%/87% in the required number of reflections.

Finally, in Figure 3, we display a comparison of (a) the Neumann series, (b) the stable implementation of our Krylov subspace approach based on decomposition (34) and (35), and (c) Kirchhoff preconditioning of the latter. Note precisely that (c) is based on the Krylov subspace iterations (described in section 5) applied to the truncated version (40) of preconditioned form (37) of the multiple scattering problem (6) utilizing the Kirchhoff operator \mathcal{K} . In our implementations we have taken N=M in (40) and used N=12/40 for the circular/elliptical configurations in Figure 1. As depicted in Figure 3, in both cases only three ORTHODIR iterations are sufficient to obtain 3-digits of accuracy which would require 20/100 iterations if the Neumann

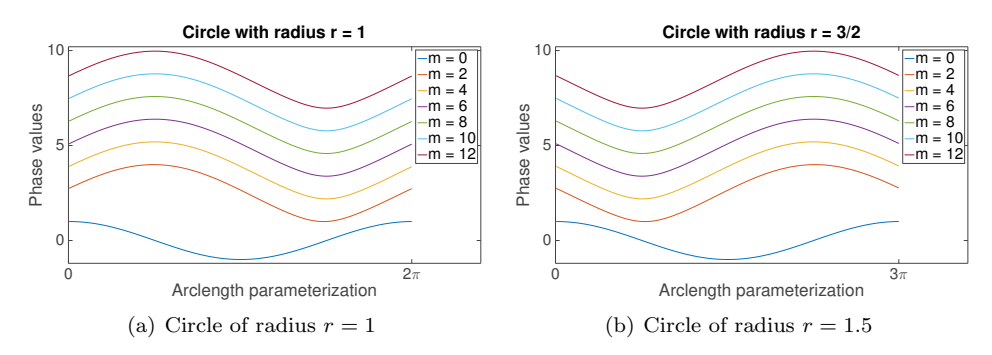


FIG. 4. Values of phase functions plotted against arclength parameterization for (periodic) reflections m=0,2,4,6,8,10,12 related with the circles of radii r=1 (left) and r=1.5 (right) in the left of Figure 1.

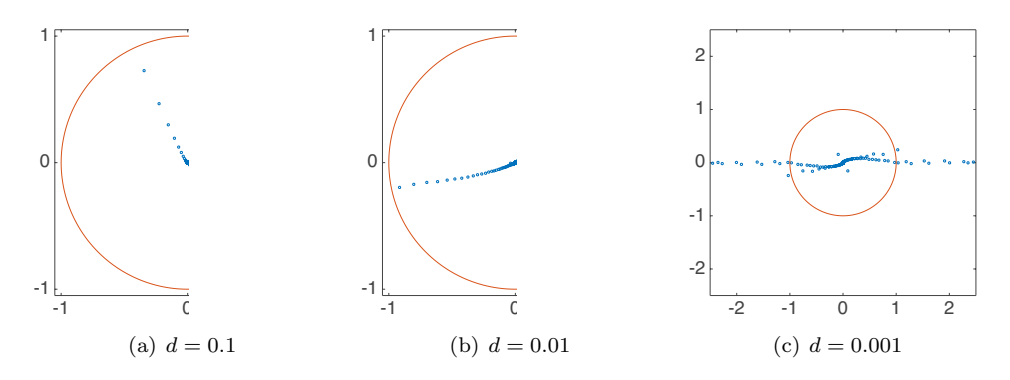
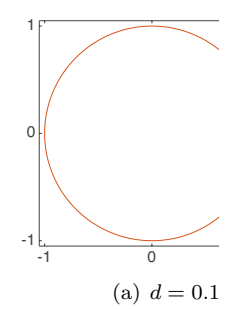
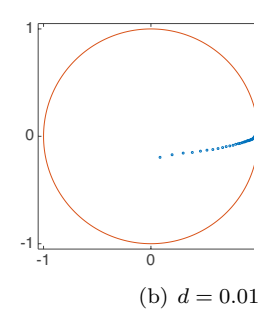


Fig. 5. The distribution of the eigenvalues in the complex plane for the operator \mathcal{T} depending on the separation distance d between two unit circles; k = 400.

series is directly used. The fact that the error does not attain the machine precision is due to the truncation of the series used to compute the preconditioner (N=12/40). Obviously inclusion of more terms yields better accuracy but at the expense of slightly more expensive numerics.

It is well known that the differences of phases associated with periodic reflections converge, as the number of iterations m goes to infinity, with a geometric rate to twice the distance between the obstacles for two periodic orbits and to the "periodic distance" for larger periodic orbits (cf. [20, 5]). It is therefore conceivable that the performance of the Neumann series and the modified Krylov method with or without the Kirchhoff preconditioner depend on this "stabilization" of the periodic phases (cf. Figure 4). However, as we can see even with this stabilization the Neumann series slowly converges in contrast with the new Krylov method with or without the Kirchhoff preconditioner (see Figures 2 and 3). Although this slow convergence of the Neumann series can be easily explained based on the rate of convergence formulas in Theorem 3, an additional problem arises at the numerical level as the distance between the obstacles decreases. Indeed, as Figure 5 displays, the distribution of the eigenvalues of (the discretized version of) the operator \mathcal{T} in the complex plane depends on the separation distance between the obstacles and overflows the unit circle with decreasing distances. On the other hand, as depicted in Figure 6, the distribution of the eigenvalues of the operator $\mathcal{I} - \mathcal{T}$ works in favor of the Krylov subspace methods since they are clustered around 1 even when the separation distance between the obstacles decreases.





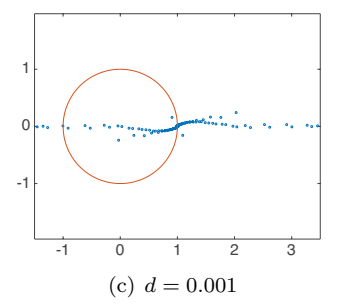


FIG. 6. The distribution of the eigenvalues in the complex plane for the operator $\mathcal{I}-\mathcal{T}$ depending on the separation distance d between two unit circles; k=400.

Table 1

Number of iterations needed for the convergence of the modified ORTHODIR algorithm and the related times for the circler configuration (left) and elliptical configuration (right).

k	ORTH iter	Time (s)
400	14	9
800	15	10
1200	15	11
1600	15	13
2000	15	14

k	ORTH iter	Time (s)
400	32	35
800	39	37
1200	45	40
1600	48	44
2000	50	46

Table 2

Number of iterations needed for the convergence of the modified ORTHODIR algorithm coupled with the Kirchhoff preconditioner and the related times for the circler configuration (left) and elliptical configuration (right).

k	Prec. ORTH iter	Time (s)
400	9	7
800	11	8
1200	11	8
1600	12	11
2000	12	11

k	Prec. ORTH iter	Time (s)
400	18	25
800	22	27
1200	23	28
1600	23	30
2000	24	32

In the next set of numerical experiments we continue with the same configuration of circles and ellipses in Figure 1, and we test our modified Krylov method for higher values of k, namely, k = 400, 800, 1200, 1600, and 2000. Since we do not have access to a reasonable approximate solution that can be computed through use of a classical solver for larger values of k, we only compute the number of iterations necessary to obtain a residual of 10^{-4} . In all the implementations, the number of discretization points used on the surface of each circle/ellipse is 400/800; note that the circumferences of ellipses are more than two times those of the circles. The obtained results are summarized in Table 1. We can observe that the number of iterations required by the modified Krylov method is clearly bounded as $k \to \infty$. For the coupling of our modified Krylov method with the dynamical Kirchhoff preconditioning, the associated numerical tests for the same range of values of k are presented in Table 2. As this table depicts, although there is a good improvement in the number of iterations in both cases, that related with computational times is not significant for circles but notable for ellipses. The number of iterations can be further reduced if we increase the number M retained in the Kirchhoff approximation (39); however, this will require more computational time.

Table 3

Number of iterations needed for the convergence of the modified ORTHODIR algorithm and its preconditioning through use of Kirchhoff approximations and the related times for N_o unit circles; k = 800.

N_o	ORTH iter	Time (s)	Prec. ORTH iter	Time (s)
4	19	21	14	12
12	32	168	21	121
20	39	214	25	197
28	45	305	32	270
36	49	418	34	357
44	51	675	35	589

Table 4

Number of iterations needed for the convergence of the modified ORTHODIR algorithm and its preconditioning through use of Kirchhoff approximations and the related times for N_o ellipses; k = 800.

N_o	ORTH iter	Time (s)	Prec. ORTH iter	Time (s)
4	11	61	14	12
12	26	180	19	127
20	39	265	26	203
28	45	346	33	282
36	48	485	33	374
44	50	674	33	599

In the following, we test the modified Krylov subspace method and the Kirchhoff preconditioner in the case of several obstacles. Specifically, we consider families of obstacles consisting of $N_0 = 4, 12, 20, 28, 36, 44$ circles and the same numbers of ellipses obtained by translations and rotations of an ellipse with major and minor axes 2.7 and 0.9. All the configurations are designed to allow for ray tracing in the sense that the convex hull of any two obstacles does not meet with any other and contain a pair of nearby obstacles. On each obstacle the number of discretization points used to implement the generalized versions of high frequency integral equations (30) and (31) (see [20, 5]) is chosen to be 200 and is independent of the wavenumber k. Note that a standard approach would require about $10 \times k$ points per obstacle, which corresponds to 10 points per wavelength $\lambda = 2\pi/k$, and result in $10 \times k \times N_o$ unknowns which can easily exceed hundreds of thousands or even millions. Tables 3 and 4 display the number of iterations necessary to attain a residual of 10^{-4} for the modified Krylov subspace method and its preconditioning for the wavenumber k = 800. Again, similar observations can be done regarding the number of iterations and the computational times. We note that surprisingly the number of necessary iterations stabilize after a certain number of scatterers in particular in the case of ellipses.

8. Conclusion. We have developed an acceleration strategy for the solution of multiple scattering problems based on a novel and effective use of the Krylov subspace method that retains the phase information and provides significant savings in computational times. Further, we have coupled this approach with an original preconditioning strategy based upon Kirchhoff approximations that greatly reduces the number of iterations needed to obtain a prescribed accuracy. However, although this preconditioner greatly enhances the convergence of the Krylov subspace method, its utilization requires some numerical optimization in order to reduce the computational time. This issue will be addressed in a forthcoming work as well as extension of these techniques to three-dimensional configurations.

REFERENCES

- T. ABBOUD, J.-C. NÉDÉLEC, AND B. ZHOU, Méthode des équations intégrales pour les hautes fréquences, C. R. Acad. Sci. Paris, 318 (1994), pp. 165–170.
- [2] T. ABBOUD, J.-C. NÉDÉLEC, AND B. ZHOU, Improvement of the integral equation method for high frequency problems, in Mathematical and Numerical Aspects of Wave Propagation: Mandelieu-La Napoule, SIAM, Philadelphia, 1995, pp. 178–187.
- [3] M. ABRAMOWITZ AND I. STEGUN, Handbook of Mathematical Functions with Formulas, Graphs, and Mathematical Tables, Martino Fine Books, Eastford, CT, 2014.
- [4] S. Amini and A. Profit, Multi-level fast multipole solution of the scattering problem, Eng. Anal. Bound. Elem., 27 (2003), pp. 547–564.
- [5] A. Anand, Y. Boubendir, F. Ecevit, and F. Reitich, Analysis of multiple scattering iterations for high-frequency scattering problems. II. The three-dimensional scalar case, Numer. Math., 114 (2010), pp. 373–427.
- [6] X. Antoine, Advances in the on-surface radiation condition method: Theory, numerics and applications, in Computational Methods for Acoustics Problems, F. Magoules, ed., Saxe-Coburg, Stirlingshire, UK, 2008, pp. 207–232.
- [7] M. BALABANE, Boundary decomposition for Helmholtz and Maxwell equations. I. Disjoint subscatterers, Asymptot. Anal., 38 (2004), pp. 1–10.
- L. Banjai and W. Hackbusch, Hierarchical matrix techniques for low- and high-frequency Helmholtz problems, IMA J. Numer. Anal., 28 (2008), pp. 46-79.
- [9] D. Boffi, Finite element approximation of eigenvalue problems, Acta Numer., 19 (2010), pp. 1– 120.
- [10] O. P. Bruno and C. A. Geuzaine, An O(1) integration scheme for three-dimensional surface scattering problems, J. Comput. Appl. Math., 204 (2007), pp. 463–476.
- [11] O. P. Bruno, V. Domínguez, and F.-J. Sayas, Convergence analysis of a high-order Nyström integral-equation method for surface scattering problems, Numer. Math., 124 (2013), pp. 603–645.
- [12] O. P. Bruno and L. A. Kunyansky, A fast, high-order algorithm for the solution of surface scattering problems: Basic implementation, tests and applications, J. Comput. Phys., 169 (2001), pp. 80–110.
- [13] O. P. Bruno, C. A. Geuzaine, J. A. Monroe, and F. Reitich, Prescribed error tolerances within fixed computational times for scattering problems of arbitrarily high frequency: The convex case, Philos. Trans. Roy. Soc. London, 362 (2004), pp. 629–645.
- [14] O. P. Bruno, C. A. Geuzaine, and F. Reitich, On the O(1) solution of multiple-scattering problems, IEEE Trans. Magn., 41 (2005), pp. 1488–1491.
- [15] S. N. CHANDLER-WILDE AND P. MONK, Wave-number-explicit bounds in time-harmonic scattering, SIAM J. Math. Anal., 39 (2008), pp. 1428–1455.
- [16] D. COLTON AND R. Kress, Inverse Acoustic and Electromagnetic Scattering Theory, Springer, Berlin, 1992.
- [17] R. W. DAVIES, K. MORGAN, AND O. HASSAN, A high order hybrid finite element method applied to the solution of electromagnetic wave scattering problems in the time domain, Comput. Mech., 44 (2009), pp. 321–331.
- [18] V. Domínguez, I. G. Graham, and V. P. Smyshlyaev, A hybrid numerical-asymptotic boundary integral method for high-frequency acoustic scattering, Numer. Math., 106 (2007), pp. 471–510.
- [19] F. ECEVIT AND H. Ç. ÖZEN, Frequency-adapted Galerkin boundary element methods for convex scattering problems, Numer. Math., 135 (2017), pp. 27–71.
- [20] F. ECEVIT AND F. REITICH, Analysis of multiple scattering iterations for high-frequency scattering problems. I. The two-dimensional case, Numer. Math., 114 (2009), pp. 271–354.
- [21] B. ENGQUIST AND A. MAJDA, Absorbing boundary conditions for the numerical simulation of waves, Math. Comp., 31 (1977), pp. 629-651.
- [22] B. ENGQUIST AND L. YING, Sweeping preconditioner for the Helmholtz equation: Moving perfectly matched layers, Multiscale Model. Simul., 9 (2011), pp. 686-710.
- [23] M. V. Fedoryuk, The stationary phase method and pseudodifferential operators, Russian Math Surveys, 26 (1971), pp. 65–115.
- [24] E. GILADI, An asymptotically derived boundary element method for the Helmholtz equation in high frequencies, J. Comput. Appl. Math., 198 (2007), pp. 52–74.
- [25] Z. GIMBUTAS AND L. GREENGARD, Fast multi-particle scattering: A hybrid solver for the Maxwell equations in microstructured materials, J. Comput. Phys., 232 (2013), pp. 22– 32
- [26] D. GIVOLI, High-order local non-reflecting boundary conditions: A review, Wave Motion, 39 (2004), pp. 319–326.

- [27] M. J. GROTE AND C. KIRSCH, Nonreflecting boundary conditions for time-dependent multiple scattering, J. Comput. Phys., 221 (2007), pp. 41–62.
- [28] M. GROTE AND I. SIM, Local nonreflecting boundary condition for time-dependent multiple scattering, J. Comput. Phys., 230 (2011), pp. 3135–3154.
- [29] J. S. HESTHAVEN AND T. WARBURTON, High-order accurate methods for time-domain electromagnetics, CMES Comput. Model. Eng. Sci., 5 (2004), pp. 395–408.
- [30] L. HÖRMANDER, Pseudo-differential operators and hypoelliptic equations. Singular integrals, Proc. Sympos. Pure Math. 10, AMS, Providence, RI, 1967, pp. 138–183.
- [31] L. HÖRMANDER, Fourier integral operators. I, Acta Math., 127 (1971), pp. 79–183.
- [32] D. HUYBRECHS AND S. VANDEWALLE, A sparse discretization for integral equation formulations of high frequency scattering problems, SIAM J. Sci. Comput., 29 (2007), pp. 2305–2328.
- [33] V. I. LEBEDEV, An Introduction to Functional Analysis in Computational Mathematics, Birkhäuser, Boston, 1997.
- [34] Y. Saad, Iterative Methods for Sparse Linear Systems, SIAM, Philadelphia, 2003.
- [35] C. C. Stolk, An improved sweeping domain decomposition preconditioner for the Helmholtz equation, Adv. Comput. Math., 43 (2017), pp. 45–76.
- [36] M. S. Tong and W. C. Chew, Multilevel fast multipole acceleration in the Nyström discretization of surface electromagnetic integral equations for composite objects, IEEE Trans. Antennas and Propagation, 58 (2010), pp. 3411–3416.
- [37] L. ZEPEDA-NÚÑEZ AND L. DEMANET, Nested domain decomposition with polarized traces for the 2D Helmholtz equation, SIAM J. Sci. Comput., to appear.